The University of Tehran Press

Pollution

Print ISSN: 2383-451X
Online ISSN: 2383-4501

https://jpoll.ut.ac.ir/

Numerical Simulation of Oil Spill Movement on Makran Coast Using Combination of Finite Volume Modeling and GNOME

Neda Mirabzadeh[1] | Mehrnaz Farzingohar[2] ✉ | Masoud Sadrinasab[3]

1. PhD Student, Department of Non Living, Atmospheric and Marine Science, University of Hormozgan, P.O.Box 79161-93145, Bandar Abbas, Iran
2. Department of Non Living, Atmospheric and Marine Science, University of Hormozgan P.O.Box 79161-93145, Bandar Abbas, Iran
3. Department of Environmental Engineering, University of Tehran, P.O.Box 14155-6135, Tehran, Iran

Article Info

Article type:
Research Article

Article history:
Received: 10 July 2024
Revised: 2 February 2025
Accepted: 1 June 2025

Keywords:
Numerical simulation
Oil spill
Finite volume
GNOME
Modeling

ABSTRACT

The finite volume method is one of the mathematical ways that was applied for tracking oil spills along the Makran coast. The GNOME model was used for comparison and validation of the calculation results. After deriving the governing equations and boundary conditions, the area is meshed for suitable accuracy, and flow data was obtained from NOAA's Real-Time Ocean Forecast System (RTOFS) for 90 days (2160 hours). Four locations were selected: one(first) point near the Strait of Hormuz, two points (second and third) near bays on the Makran coast, and another (forth) near the Pakistan border. At each point, 1000 liters of Medium Crude Oil were released. Results showed that the currents in the Hormuz Strait had a significant impact on the first point, and the pollution spread over two-thirds of Makran's coast within three months. The second and third points affected the coastlines inside the bays, while the fourth point showed pollution spreading toward Pakistan's coast. The results were compared with GNOME, and the average differences for all the locations were 92.33%, 92.28%, 91.03%, and 92.40%, respectively.

Cite this article: Mirabzadeh, N., Farzingohar, M., & Sadrinasab, M. (2025). Numerical Simulation of Oil Spill Movement on Makran Coast Using Combination of Finite Volume Modeling and GNOME. *Pollution*, 11(3), 609-629. https://doi.org/10.22059/poll.2025.378543.2456

DOI: https://doi.org/10.22059/poll.2025.378543.2456

INTRODUCTION

Oil spills, influenced by gravity, surface tension, viscosity, and buoyancy, cause thin layers to spread over vast areas (A. Drozdowski et al.,2011). Key factors in spills are the oil's thickness and the contaminated area's size (S. Venkatesh et al.,1990). Notable models in this field include Fai's work, highlighting surface tension, inertia, and viscosity (JA Fay,1969), and McKay et al.'s circular release prediction (D. Mackay et al.,1982). Oil spill models aim to forecast the spill's movement using data like ocean currents and winds (M.Afenyo et al.,2016) These models integrate three components: input data, climate information, and diffusion algorithms, producing outputs for spill behavior (M.Yang et al.,2015) Several modeling programs like SIMAP/OILMAP, GNOME, and COSIM focus on both surface and subsurface processes (DP French-McCay et al.,2017 & JS Camp et al.,2010) . Research in Spain showed statistical models' value for spill response planning (AJ Abascal et al.,2010). Chao et al.'s two-

*Corresponding Author Email: *farzingohar@hormozgan.ac.ir*

dimensional model and Wang et al.'s two-layer model addressed oil's behavior considering temperature, currents, and evaporation (X.Chao et al.,2001 & S.Wang et al.,2005). Saywell et al. used a Lagrangian model to track surface spills with a focus on accumulation probabilities (JM Sayol et al.,2014). In contrast, Talish's constant Eulerian model applied Navier-Stokes equations to simulate oil dynamics (P.Tkalich,2006). Agrawal and Dakshinamothy used a CFD-based approach, noting significant impacts from ocean conditions on oil spread (M. Agrawal & D. Dakshinamoorthy,2011). A study in Tokyo Bay showed good alignment between model predictions and satellite data (S-i. Sugioka,1999). Simic and Liher stressed the importance of understanding physical processes for predicting pollutant movement (D. Simecek-Beatty & WJ Lehr,2007). Basar et al. highlighted currents' stronger influence over wind on oil spills (E. Basar, E. Kose, & A. Guneroglu, 2006). Modeling oil spill diffusion involves complex factors (CAD Fraga Filho,2021 & H. Abbasi & R. Lubbad,2021). Separate phase models struggle to integrate both horizontal spread and water column dispersion, a limitation leading to a preference for multi-phase models (M. Raznahan et al.,2021 & C-T. Ha & JH Lee,2020). These models allow simultaneous assessment of oil distribution phases, showing interactions(Z. Zhang et al.,2020). In another study several scenarios with different seasonal atmospheric and oceanic data of oil pollution are molded by GNOME in Perian Gulf along Qeshm Channel showed the wind and channel boundaries are impacted to the spill distribution (Farzingohar et al.,2024).

The development of a numerical method that simultaneously addresses all phases of oil distribution and transfer is rarely found in existing literature. Additionally, creating an effective numerical model to predict oil spill behavior requires accurate boundary conditions. These conditions are not only influenced by weather factors such as radiation and precipitation but are also shaped by statistical variables. Therefore, combining these approaches can lead to a more precise prediction of oil spill dynamics.

MATERIALS AND METHODS

The coastal area of the North Sea of Oman or Makran is considered as one of the most important water areas in the world in terms of biodiversity, fishery resources and especially rich oil resources, a unique ecosystem (M. A. Ahrari Roudi, 2021). However, with the increase in transportation operations, oil pollution received special attention. Millions of petroleum products enter coastal and marine environments from various sources. According to available studies and reports, half a million tons of oil are continuously discharged into the sea every year (MA Zahed et al.,2010) Considering the destructive effects of oil pollution on the sea ecosystem and coastal areas, identifying and predicting the path of oil pollution in the event of an accident is of great importance. A well-known solution in estimating the surface path of oil spills and coastal protection is the use of modeling and simulations of oil spills (D. Yousefi Kobriya et al.,2020).

Governing Equation

The finite volume method is one of the numerical methods for the approximate solution of differential equations. The finite volume method is actually a type of finite element method in which the approximation method of these integrals is different from the finite element method. In other words, the finite volume method is a combination of the finite difference method and the finite element method, which is chosen according to the conditions of the Makran coast (flow discontinuity, etc.) to solve the equations. Due to the fact that climate changes on the coasts and bays cause oil pollution to spread faster on the surface (F. Qiao et al.,2019), therefore, to increase the accuracy of the control volume calculations, the metric coefficients $h_1.h_1.\ h_2h_2$ which increased the accuracy of calculations during finite volume integration for momentum

and similar equations. Based on the recommended control volume is:

$$h_1\delta x_1 = \ddot{A}x_1 \;\&\; h_2\delta x_2 = \ddot{A}x_2 \tag{1}$$

The length of a segment in the control volume is calculated by the following equation:

$$ds^2 = \left(h_1 dx_1\right)^2 + \left(h_2 dx_2\right)^2 + dz^2 \tag{2}$$

The continuity equation is written as follows:

$$\frac{\partial \mathrm{u}}{\partial \mathrm{x}} + \frac{\partial \mathrm{v}}{\partial \mathrm{y}} + \frac{\partial \mathrm{w}}{\partial \mathrm{z}} = 0 \tag{3}$$

Which according to the metric coefficients, it is rewritten as follows:

$$\frac{\partial}{\partial x_1}\left(h_2 u_1\right) + \frac{\partial}{\partial x_2}\left(h_1 u_2\right) + h_1 h_2 \frac{\partial w}{\partial z} = 0 \tag{4}$$

where u_1 and u_2 are the speed in x and y directions. To derive other equations with the following assumptions:

· The fluid is incompressible.

· Variations on the density of the Boussinesq estimate (floating).

The general form of momentum equations is written as follows:

$$\begin{aligned}
&\frac{\partial \mathrm{u}}{\partial \tilde{n}} + \mathrm{u}\frac{\partial \mathrm{u}}{\mathrm{x}\partial \mathrm{x}} + \mathrm{v}\frac{\partial \mathrm{u}}{\mathrm{z}\partial \mathrm{y}} + \mathrm{w}\frac{\partial \mathrm{u}}{\mathrm{z}\partial \mathrm{z}} - \mathrm{fv} = -\frac{1}{{}_0}\frac{\partial \mathrm{P}}{\partial} + \frac{\partial}{\partial}\left(\mathrm{K_m}\frac{\partial \mathrm{u}}{\partial}\right) + \mathrm{F_u} \\
&\frac{\partial \mathrm{v}}{\partial \tilde{n}} + \mathrm{u}\frac{\partial \mathrm{v}}{\mathrm{y}\partial \mathrm{x}} + \mathrm{v}\frac{\partial \mathrm{u}}{\mathrm{z}\partial \mathrm{y}} + \mathrm{w}\frac{\partial \mathrm{v}}{\mathrm{z}\partial \mathrm{z}} - \mathrm{fu} = -\frac{1}{{}_0}\frac{\partial \mathrm{P}}{\partial} + \frac{\partial}{\partial}\left(\mathrm{K_m}\frac{\partial \mathrm{v}}{\partial}\right) + \mathrm{F_v}\ \frac{\partial \mathrm{v}}{\partial \mathrm{z}} = -\tilde{n}\mathrm{g}
\end{aligned} \tag{5}$$

Which is rewritten as follows according to the metric coefficients:

$$\begin{aligned}
&\frac{\partial u_1}{\partial t} + \frac{1}{h_1 h_2}\left[\frac{\partial}{\partial x_1}\left(h_2 u_1^2\right) + \frac{\partial}{\partial x_2}\left(h_1 u_1 u_2\right)\right] + \frac{\partial}{\partial z}\left(w u_1\right) + \\
&\frac{u_1 u_2}{h_1 h_2}\frac{\partial h_1}{\partial x_2} - \frac{u_2^2}{h_1 h_2}\frac{\partial h_2}{\partial x_1} - f u_2 = -\frac{1}{\rho_0 h_1}\frac{\partial P}{\partial x_1} \\
&+\frac{1}{h_1 h_2}\left[\frac{\partial}{\partial x_1}\left(h_2 \tau_{12}\right) + \frac{\partial}{\partial x_2}\left(h_1 \tau_{22}\right) + \tau_{12}\frac{\partial h_2}{\partial x_2} - \tau_{11}\frac{\partial h_1}{\partial x_2}\right] + \frac{\partial}{\partial z}\left(\mathrm{K}_M \frac{\partial u_1}{\partial z}\right)
\end{aligned} \tag{6}$$

$$\begin{aligned}
&\frac{\partial u_2}{\partial t} + \frac{1}{h_1 h_2}\left[\frac{\partial}{\partial x_1}\left(h_2 u_1 u_2\right) + \frac{\partial}{\partial x_2}\left(h_2 u_2^2\right)\right] + \frac{\partial}{\partial z}\left(w u_2\right) + \frac{u_1 u_2}{h_1 h_2}\frac{\partial h_2}{\partial x_1} - \frac{u_1^2}{h_1 h_2}\frac{\partial h_1}{\partial x_2} - f u_1 = \\
&-\frac{1}{\rho_0 h_2}\frac{\partial P}{\partial x_2} + \frac{1}{h_1 h_2}\left[\frac{\partial}{\partial x_1}\left(h_2 \tau_{12}\right) + \frac{\partial}{\partial x_2}\left(h_1 \tau_{22}\right) + \tau_{12}\frac{\partial h_2}{\partial x_2} - \tau_{11}\frac{\partial h_1}{\partial x_2}\right] + \frac{\partial}{\partial z}\left(\mathrm{K}_M \frac{\partial u_2}{\partial z}\right)
\end{aligned} \tag{7}$$

The pressure distribution is:

$$\frac{\rho}{\rho_0} g = -\frac{1}{\rho_0}\frac{\partial P}{\partial z} \tag{8}$$

In the above equations, ρ is the density, ρ_0 is the reference density, g is the gravitational acceleration of the Earth, P is the pressure, f is the Coriolis parameter equivalent to f=2Ωsinϕ, where Ω is the angular velocity of the Earth in radians per second and ϕ is the latitude, of course, only the vertical component of the Coriolis acceleration. It is meant in the equations and K_M is permeability in the vertical direction and τ_{11} τ_{22} and τ_{12} are the Reynolds stress tensor components in the symmetric state which are defined by the following formulas:

$$\tau_{11} = 2\mathrm{A}_M \left[\frac{1}{h_1}\frac{\partial u_1}{\partial x_1} + \frac{u_2}{h_1 h_2}\frac{\partial h_1}{\partial x_2} \right] \tag{9}$$

$$\tau_{12} = \mathrm{A}_M \left[\frac{h_1}{h_2}\frac{\partial}{\partial x_2}\left(\frac{u_1}{h_1}\right) + \frac{h_2}{h_1}\frac{\partial}{\partial x_1}\left(\frac{u_2}{h_2}\right) \right] = \tau_{21} \tag{10}$$

$$\tau_{22} = 2\mathrm{A}_M \left[\frac{1}{h_2}\frac{\partial u_2}{\partial x_2} + \frac{u_1}{h_1 h_2}\frac{\partial h_2}{\partial x_1} \right] \tag{11}$$

That A_M is permeability in the horizontal direction. It should be noted that in equation (8), the pressure value is obtained by the following integral:

$$\mathrm{P} = \mathrm{P}_a + \rho_0 g\eta + g\int_z \rho(\xi)\, d\xi \tag{12}$$

Where P_a the atmospheric pressure and η is the height above the free surface of the sea water. Which is a suitable estimate for simulating the atmospheric pressure on the sea surface. When oil is spilled on the surface of the sea, it spreads in the form of a thin layer. The movement of the oil spill depends on the transmission and distribution factors that are caused by currents, waves and wind. Since the composition of the oil changes from the initial time of the leak, due to the balance between the forces of gravity, viscosity and surface tension, the oil stain spreads on the surface of the water. Volatile parts evaporate, water-soluble components dissolve in the water column, and insoluble components are suspended and dispersed in the form of small droplets in the water column. Surface tension spreads on the surface of calm sea waters. After a short period of time, the gravitational force is negligible compared to the surface tension force, and the spreading action continues until the viscosity overcomes the spreading force. Transfer of spilled oil is basically based on the following factors:

- Spreading of oil spill due to the forces of gravity, inertia, viscosity and surface tension
- Net transmission and spread of horizontal turbulence caused by water flow and wind
- Evaporation and decomposition caused by weather processes
- Vertical propagation caused by wave breaking and disturbance of the upper layer

Therefore, the multi-component mixture, whose density is a complex function of temperature, components such as seawater and oil spill, and pressure (a function of z), is (W. Lehr et al,.2002

& AT Hoang et al,.2018).In order to properly calculate the density in oil spill contamination, usually the pressure term is considered as part of the internal characteristics of the density, which is called potential density. The remaining terms will consist of components such as seawater and oil spill(R. Smith et al,2014).

$$\rho = \rho(\Theta, S_i), \tag{13}$$

In the above equation, Θ is the potential temperature and S_i is components such as sea water and oil spill components. i is the index of the component according to the said definition. Therefore, the mass conservation equations in this case are generally as follows:

$$\frac{\partial \theta}{\partial t} + u\frac{\partial \theta}{\partial x} + v\frac{\partial \theta}{\partial y} + w\frac{\partial \theta}{\partial z} = \frac{\partial}{\partial z}\left(K_H \frac{\partial \theta}{\partial z}\right) + F_\theta \tag{14}$$

$$\frac{\partial s}{\partial t} + u\frac{\partial s}{\partial x} + v\frac{\partial s}{\partial y} + w\frac{\partial s}{\partial z} = \frac{\partial}{\partial z}\left(K_H \frac{\partial s}{\partial z}\right) + F_s$$

According to the metric coefficients, as:

$$\frac{\partial \Theta}{\partial t} + \frac{1}{h_1 h_2}\left[\frac{\partial}{\partial x_1}(h_2 u_1 \Theta) + \frac{\partial}{\partial x_2}(h_1 u_2 \Theta)\right] + \frac{\partial}{\partial z}(w\Theta) = \frac{1}{h_1 h_2}\left[\frac{\partial}{\partial x_1}\left(A_H \frac{h_2}{h_1}\frac{\partial \Theta}{\partial x_1}\right) + \frac{\partial}{\partial x_2}\left(A_H \frac{h_1}{h_2}\frac{\partial \Theta}{\partial x_2}\right)\right] + \frac{\partial}{\partial z}\left(K_H \frac{\partial \Theta}{\partial z}\right) + \frac{\partial Q_S}{\partial z} \tag{15}$$

$$\frac{\partial S_i}{\partial t} + \frac{1}{h_1 h_2}\left[\frac{\partial}{\partial x_1}(h_2 u_1 S_i) + \frac{\partial}{\partial x_2}(h_1 u_2 S_i)\right] + \frac{\partial}{\partial z}(w S_i) = \frac{1}{h_1 h_2}\left[\frac{\partial}{\partial x_1}\left(A_H \frac{h_2}{h_1}\frac{\partial S_i}{\partial x_1}\right) + \frac{\partial}{\partial x_2}\left(A_H \frac{h_1}{h_2}\frac{\partial S_i}{\partial x_2}\right)\right] + \frac{\partial}{\partial z}\left(K_H \frac{\partial S_i}{\partial z}\right) \tag{16}$$

In the above equations, K_H is the eddy permeability in the vertical direction and A_H is the eddy permeability in the horizontal direction for a water column in the turbulent mixing of heat and oil spill, and $\frac{\partial Q_S}{\partial z}$ is the heat based on solar radiation. Now, according to (GL Mellor & T. Yamada,.1982), the equations of turbulent flow are generally:

$$\frac{\partial q^2}{\partial t} + u\frac{\partial q^2}{\partial x} + v\frac{\partial q^2}{\partial y} + w\frac{\partial q^2}{\partial z} = 2(P_s + P_b + \varepsilon) + \frac{\partial}{\partial z}\left(K_q \frac{\partial q^2}{\partial z}\right) + F_q$$

$$\frac{\partial q^2 l}{\partial t} + u\frac{\partial q^2 l}{\partial x} + v\frac{\partial q^2 l}{\partial y} + w\frac{\partial q^2 l}{\partial z} = lE_1\left(P_s + P_b + \frac{\widetilde{W}}{E_1}\varepsilon\right)\frac{\partial}{\partial z}\left(K_q \frac{\partial q^2 l}{\partial z}\right) + F_q \tag{17}$$

Which will be the same as before after conversion as follows:

$$\frac{\partial}{\partial t}\left(q^2\right)+\frac{1}{h_1h_2}\left[\frac{\partial}{\partial x_1}\left(h_2u_1q^2\right)\frac{\partial}{\partial x_2}\left(h_1u_2q^2\right)\right]+\frac{\partial}{\partial z}\left(wq^2\right)=2\mathrm{K_M}\left[\left(\frac{\partial u_1}{\partial z}\right)^2+\left(\frac{\partial u_2}{\partial z}\right)^2\right]+$$
$$2\mathrm{K_H}\frac{g}{\rho 0}\frac{\partial\rho}{\partial z}-\frac{2q^3}{\mathrm{B_1}l}+\frac{1}{h_1h_2}\left[\frac{\partial}{\partial x_1}\left(\mathrm{A_H}\frac{h_2}{h_1}\frac{\partial q^2}{\partial x_1}\right)+\frac{\partial}{\partial \chi_2}\left(\mathrm{A_H}\frac{h_1}{h_2}\frac{\partial q^2}{\partial x_2}\right)\right]+\frac{\partial}{\partial z}\left(K_q\frac{\partial q^2}{\partial z}\right) \quad (18)$$

$$\frac{\partial}{\partial t}\left(q^2l\right)+\frac{1}{h_1h_2}\left[\frac{\partial}{\partial x_1}\left(h_2u_1q^2l\right)\frac{\partial}{\partial x_2}\left(h_1u_2q^2l\right)\right]+\frac{\partial}{\partial z}\left(wq^2\right)=\mathrm{K_M}E_1l\left[\left(\frac{\partial u_1}{\partial z}\right)^2+\left(\frac{\partial u_2}{\partial z}\right)^2\right]+ \quad (19)$$
$$\mathrm{K_H}E_3l\frac{g}{\rho 0}\frac{\partial\rho}{\partial z}-\frac{q^3}{\mathrm{B_1}}\left[1+E_2\left(\frac{l}{\kappa\, L}\right)^2\right]+\frac{1}{h_1h_2}\left[\frac{\partial}{\partial x_1}\left(\mathrm{A_H}\frac{h_2}{h_1}\frac{\partial}{\partial x_1}\left(q^2l\right)\right)+\frac{\partial}{\partial x_2}\left(\mathrm{A_H}\frac{h_1}{h_2}\frac{\partial}{\partial x_2}\left(q^2l\right)\right)\right]+\frac{\partial}{\partial z}\left(K_q\frac{\partial}{\partial z}\left(q^2l\right)\right)$$

In the equations (19), $q^2/2$ the amount of kinetic energy and l the magnitude of the entangled current, the coefficients $\mathrm{K_M}$, $\mathrm{K_H}$, and K_q, which are related to the permeability of the entangled state, obtained as equation(20) (B. Galperin et al.,1988):

$$\mathrm{K_M}=lqS_\mathrm{M},\ \ \mathrm{K}_H=lqS_H,\ \ \mathrm{K}_q=lqS_q \quad (20)$$

S_M, S_HS_q are stability functions that are calculated with the below as:

$$S_M=A_1\left[\frac{\left(1-\frac{6A_1}{B_1}-3C_1\right)+9\left(2A_1+A_2\right)S_HG_H}{\left(1-9A_1A_2G_H\right)}\right] \quad (21)$$

$$S_H=A_2\left[\frac{1-\frac{6A_1}{B_1}}{1-3A_2G_H\left(6A_1+B_2\right)}\right] \quad (22)$$

$$S_q=0.2 \quad (23)$$

$$G_H=\frac{l^2}{q^2}\frac{g}{\rho 0}\frac{\partial\rho}{\partial z} \quad (24)$$

Hence A_1, A_2, B_1, B_2 are constants that show the ratio of the change in the length of the entangled current to the magnitude of the entangled current l.

S_M and S_H are functions of G_H which are obviously related to the buoyancy gradient. The coordinate system chosen is Sigma, where the vertical coordinates of bathymetry follows and keeps the same number of vertical grid points everywhere in the domain, no matter how deep the blue column is, while the thickness of the layer varies with depth. However, sigma coordinate models are not effective when seafloor changes have abrupt slope changes because

pressure gradient errors can cause unrealistic currents.(GL Mellor et al.,2002 & NR da Silva & IH Manssour,2007). Now, according to the type of coordinate system and related theory, the relation for conversion is:

$$\sigma = \frac{z-\eta}{\mathrm{H}+\eta} \tag{25}$$

Continuity equation in sigma coordinates

$$\frac{\partial \eta}{\partial t} + \frac{1}{h_1 h_2}\left[\frac{\partial}{\partial x_1}\left(h_2 u_1 D\right) + \frac{\partial}{\partial x_2}\left(h_1 u_2 D\right)\right] + \frac{\partial \overline{w}}{\partial \sigma} = 0 \tag{26}$$

Momentum equations in sigma coordinates

$$\begin{aligned}&\frac{\partial}{\partial t}\left(u_1 D\right) + \frac{1}{h_1 h_2}\left[\frac{\partial}{\partial x_1}\left(h_2 u_1^2 D\right) + \frac{\partial}{\partial x_2}\left(h_1 u_1 u_2 D\right)\right] + \frac{\partial}{\partial \sigma}\left(\overline{w} u_1\right) + \\ &\frac{u_1 u_2 D}{h_1 h_2}\frac{\partial h_1}{\partial x_2} - \frac{u_2^2 D}{h_1 h_2}\frac{\partial h_2}{\partial x_1} - f u_2 D = -D\mathrm{P}_1 + \frac{\partial}{\partial \sigma}\left(\frac{\mathrm{K_M}}{D}\frac{\partial u_1}{\partial \sigma}\right) + DF_1\end{aligned} \tag{27}$$

$$\begin{aligned}&\frac{\partial}{\partial t}\left(u_2 D\right) + \frac{1}{h_1 h_2}\left[\frac{\partial}{\partial x_1}\left(h_2 u_1 u_2 D\right)\frac{\partial}{\partial x_2}\left(h_1 u_2^2 D\right)\right] + \frac{\partial}{\partial \sigma}\left(\overline{w} u_2\right) + \\ &\frac{u_1 u_2 D}{h_1 h_2}\frac{\partial h_2}{\partial x_1} - \frac{u_1^2 D}{h_1 h_2}\frac{\partial h_1}{\partial x_2} - f u_1 D = -D\mathrm{P}_2 + \frac{\partial}{\partial \sigma}\left(\frac{\mathrm{K_M}}{D}\frac{\partial u_2}{\partial \sigma}\right) + DF_2\end{aligned} \tag{28}$$

Density equations in sigma coordinates

$$\begin{aligned}&\frac{\partial}{\partial t}(\Theta D) + \frac{1}{h_1 h_2}\left[\frac{\partial}{\partial x_1}(h_2 u_1 \Theta D) + \frac{\partial}{\partial x_2}(h_1 u_2 \Theta D)\right] + \frac{\partial}{\partial \sigma}(\overline{w}\Theta) \\ &\qquad = \frac{\partial}{\partial \sigma}\left(\frac{\mathrm{K_H}}{D}\frac{\partial \Theta}{\partial \sigma}\right) + DF_\Theta\end{aligned} \tag{29}$$

$$\frac{\partial}{\partial t}\left(S_i D\right) + \frac{1}{h_1 h_2}\left[\frac{\partial}{\partial x_1}\left(h_2 u_1 S_i D\right) + \frac{\partial}{\partial x_2}\left(h_1 u_2 S_i D\right)\right] + \frac{\partial}{\partial \sigma}\left(\overline{w} S_i\right) = \frac{\partial}{\partial \sigma}\left(\frac{\mathrm{K_H}}{D}\frac{\partial S_i}{\partial \sigma}\right) + DF_{S_i} \tag{30}$$

Turbulent flow equations in sigma coordinates

$$\begin{aligned}&\frac{\partial}{\partial t}\left(q^2 D\right) + \frac{1}{h_1 h_2}\left[\frac{\partial}{\partial x_1}\left(h_2 u_1 q^2 D\right) + \frac{\partial}{\partial x_2}\left(h_1 u_2 q^2 D\right)\right] + \frac{\partial}{\partial \sigma}\left(\overline{w} q^2\right) = \\ &\frac{\partial}{\partial \sigma}\left(\frac{\mathrm{K}_p}{D}\frac{\partial q^2}{\partial \sigma}\right) + \frac{2\mathrm{K_M}}{D}\left[\left(\frac{\partial u_1}{\partial \sigma}\right)^2 + \left(\frac{\partial u_2}{\partial \sigma}\right)^2\right] + 2\mathrm{K_H}\frac{g}{\rho}\frac{\partial \rho}{\partial \sigma} - \frac{2q^3 D}{\mathrm{B}_1 l} DF_q\end{aligned} \tag{31}$$

$$\begin{aligned}&\frac{\partial}{\partial t}\left(q^2 l D\right) + \frac{1}{h_1 h_2}\left[\frac{\partial}{\partial x_1}\left(h_2 u_2 q^2 l D\right) + \frac{\partial}{\partial x_2}\left(h_1 u_2 q^2 l D\right)\right] + \frac{\partial}{\partial \sigma}\left(\overline{w} q^2 l\right) = \\ &\frac{\partial}{\partial \sigma}\left[\frac{\mathrm{K}_q}{D}\frac{\partial}{\partial \sigma}\left(q^2 l\right)\right] + \mathrm{K_M E_1}\frac{l}{D}\left[\left(\frac{\partial u_1}{\partial \sigma}\right)^2 + \left(\frac{\partial u_2}{\partial \sigma}\right)^2\right] + \mathrm{K_H E_3} l \frac{g}{\rho}\frac{\partial \rho}{\partial \sigma} - \frac{q^3 D}{\mathrm{B}_1}\left[1 + \mathrm{E}_2\left(\frac{l}{\kappa L}\right)^2\right] + DF_l\end{aligned} \tag{32}$$

Which $\overline{w}$ is vertical speed in the Sigma coordinate system expressed by the following equation:

$$\overline{w} = w - u_1\sigma\frac{\partial D}{\partial x_1} + \frac{\partial \eta}{x_1} - u_2\sigma\frac{\partial D}{\partial x_2} + \frac{\partial \eta}{\partial x_2} - \left(\sigma\frac{\partial D}{\partial t} + \frac{\partial \eta}{\partial t}\right) \tag{33}$$

$\overline{w}$ the boundary conditions for the new coordinate system are:

$$\sigma = -1, \sigma = 0 \ \rightarrow \ \overline{w} = 0 \tag{34}$$

The pressure gradient will be as follows:

$$DP_1 = \frac{D}{\rho 0}\frac{\partial p_a}{\partial x_1} + \rho D\frac{\partial \eta}{\partial \chi_1} + \frac{gD^2}{\rho 0}\left[\frac{\partial}{\partial x_1}\int_\sigma^0 \rho d\sigma' - \rho\left(\frac{\sigma}{D}\frac{\partial D}{\partial x_1} + \frac{1}{D}\frac{\partial \eta}{\partial x_1}\right)\right] - \frac{gD}{\rho 0}\frac{\partial D}{\partial x_1}\int_\sigma^0 \sigma'\frac{\partial \rho}{\partial \sigma'}d\sigma' \tag{35}$$

$$DP_2 = \frac{D}{\rho 0}\frac{\partial p_a}{\partial x_2} + \rho D\frac{\partial \eta}{\partial x_2} + \frac{gD^2}{0}\left[\frac{\partial}{\partial x_2}\int_\sigma^0 \rho d\sigma' - \rho\left(\frac{\sigma}{D}\frac{\partial D}{\partial x_2} + \frac{1}{D}\frac{\partial \eta}{\partial x_2}\right)\right] - \frac{gD}{\rho 0}\frac{\partial D}{\partial x_2}\int_\sigma^0 \sigma'\frac{\partial \rho}{\partial \sigma'}d\sigma' \tag{36}$$

It will be obtained by the following relations:

$$DF_1 = \frac{1}{h_1 h_2}\left\{\frac{\partial}{\partial x_1}(h_2\tau_{11}) - h_2\frac{\partial}{\partial \sigma}\left[\left(\frac{\sigma}{D}\frac{\partial D}{\partial x_2} + \frac{1}{D}\frac{\partial \eta}{\partial x_2}\right)\tau_{11}\right]\right\} + \frac{\partial}{\partial x_2}\left\{(h_1\tau_{21}) - h_1\frac{\partial}{\partial \sigma}\left[\left(\frac{\sigma}{D}\frac{\partial D}{\partial x_2} + \frac{1}{D}\frac{\partial \eta}{\partial x_2}\right)\tau_{21}\right] + \tau_{21}\frac{\partial h_1}{\partial x_2} - \tau_{22}\frac{\partial h_2}{\partial x_1}\right\} \tag{37}$$

$$DF_2 = \frac{1}{h_1 h_2}\left\{\frac{\partial}{\partial x_1}(h_2\tau_{12}) - h_2\frac{\partial}{\partial \sigma}\left[\left(\frac{\sigma}{D}\frac{\partial D}{\partial x_1} + \frac{1}{D}\frac{\partial \eta}{\partial x_1}\right)\tau_{12}\right]\right\} + \frac{\partial}{\partial x_2}\left\{(h_1\tau_{22}) - h_1\frac{\partial}{\partial \sigma}\left[\left(\frac{\sigma}{D}\frac{\partial D}{\partial x_2} + \frac{1}{D}\frac{\partial \eta}{\partial x_2}\right)\tau_{22}\right] + \tau_{12}\frac{\partial h_2}{\partial x_1} - \tau_{11}\frac{\partial h_1}{\partial x_2}\right\} \tag{38}$$

Whereas:

$$\tau_{11} = 2\mathrm{A_M}\left\{\frac{1}{h_1}\left[\frac{\partial}{\partial x_1}(\mu_1 D) - \frac{\partial}{\partial \sigma}\left[\mu_1\left(\sigma\frac{\partial D}{\partial x_1} + \frac{\partial \eta}{\partial \chi_1}\right)\right]\right] + \frac{\mu_2 D}{h_1 h_2}\frac{\partial h_1}{\partial x_2}\right\} \tag{39}$$

$$\tau_{12} = 2\mathrm{A_M}\left\{\frac{h_1}{h_2}\left[\frac{\partial}{\partial x_2}\left(\frac{\mu_1 D}{h_1}\right) - \frac{1}{h_1}\frac{\partial}{\partial \sigma}\left[\left(\sigma\frac{\partial D}{\partial x_2} + \frac{\partial \eta}{\partial x_2}\right)\mu_1\right]\right]\right\} + \frac{h_2}{h_1}\left[\frac{\partial}{\partial x_1}\left(\frac{\mu_2 D}{h_2}\right) - \frac{1}{h_2}\frac{\partial}{\partial \sigma}\left[\left(\sigma\frac{\partial D}{\partial x_1} + \frac{\partial \eta}{\partial x_1}\right)\mu_2\right]\right] \tag{40}$$

$$\tau_{22} = 2\mathrm{A_M}\left\{\frac{1}{h_2}\left[\frac{\partial}{\partial x_2}(\mu_2 D) - \frac{\partial}{\partial \sigma}\left(\mu_2\left(\sigma\frac{\partial D}{\partial x_2} + \frac{\partial \eta}{\partial x_2}\right)\right)\right]\frac{\mu_1 D}{h_1 h_2}\frac{\partial h_2}{\partial x_1}\right\} \tag{41}$$

Horizontal permeability are:

$$\begin{aligned} DF_\Theta = \frac{1}{h_1 h_2}\Bigg\{&\frac{\partial}{\partial x_1}(h_2 q_1) - h_2\frac{\partial}{\partial \sigma}\left[\left(\frac{\sigma}{D}\frac{\partial D}{\partial x_1} + \frac{1}{D}\frac{\partial \eta}{\partial x_1}\right)q_1\right]\Bigg\} \\ &+ \frac{\partial}{\partial x_2}\Bigg\{(h_1 q_2) - h_1\frac{\partial}{\partial \sigma}\left[\left(\frac{\sigma}{D}\frac{\partial D}{\partial x_2} + \frac{1}{D}\frac{\partial \eta}{\partial x_2}\right)q_2\right]\Bigg\} \end{aligned} \tag{42}$$

$$q_1 = \mathrm{A_H}\frac{1}{h_1}\left\{\frac{\partial}{\partial x_1}(\Theta D) - \frac{\partial}{\partial \sigma}\left[\left(\sigma\frac{\partial D}{\partial x_1} + \frac{\partial \eta}{\partial x_1}\right)\Theta\right]\right\} \tag{43}$$

$$q_2 = \mathrm{A_H}\frac{1}{h_2}\left\{\frac{\partial}{\partial x_2}(\Theta D) - \frac{\partial}{\partial \sigma}\left[\left(\sigma\frac{\partial D}{\partial x_2} + \frac{\partial \eta}{\partial x_2}\right)\Theta\right]\right\} \tag{44}$$

$$\begin{aligned} DF_{S_i} = &\frac{1}{h_1 h_2}\left\{\frac{\partial}{\partial x_1}(h_2 q_1) - h_2\frac{\partial}{\partial \sigma}\left[\left(\frac{\sigma}{D}\frac{\partial D}{\partial x_1} + \frac{1}{D}\frac{\partial \eta}{\partial x_1}\right)q_1\right]\right\} \\ &+ \frac{\partial}{\partial x_2}\left\{(h_1 q_2) - h_1\frac{\partial}{\partial \sigma}\left[\left(\frac{\sigma}{D}\frac{\partial D}{\partial x_2} + \frac{1}{D}\frac{\partial \eta}{\partial x_2}\right)q_2\right]\right\} \end{aligned} \tag{45}$$

$$q_1 = \mathrm{A_H}\frac{1}{h_1}\left\{\frac{\partial}{\partial x_1}(S_i D) - \frac{\partial}{\partial \sigma}\left[\left(\sigma\frac{\partial D}{\partial x_1} + \frac{\partial \eta}{\partial x_1}\right)S_i\right]\right\} \tag{46}$$

$$q_2 = \mathrm{A_H}\frac{1}{h_2}\left\{\frac{\partial}{\partial x_2}(S_i D) - \frac{\partial}{\partial \sigma}\left[\left(\sigma\frac{\partial D}{\partial x_2} + \frac{\partial \eta}{\partial x_2}\right)S_i\right]\right\} \tag{47}$$

$$\begin{aligned} DF_{\psi_i} = &\frac{1}{h_1 h_2}\left\{\frac{\partial}{\partial x_1}(h_2 q_1) - h_2\frac{\partial}{\partial \sigma}\left[\left(\frac{\sigma}{D}\frac{\partial D}{\partial x_1} + \frac{1}{D}\frac{\partial \eta}{\partial x_1}\right)q_1\right]\right\} \\ &+ \frac{\partial}{\partial x_2}\left\{(h_1 q_2) - h_1\frac{\partial}{\partial \sigma}\left[\left(\frac{\sigma}{D}\frac{\partial D}{\partial x_2} + \frac{1}{D}\frac{\partial \eta}{\partial x_2}\right)q_2\right]\right\} \end{aligned} \tag{48}$$

$$q_1 = \mathrm{A_H}\frac{1}{h_1}\left\{\frac{\partial}{\partial x_1}(\psi_i D) - \frac{\partial}{\partial \sigma}\left[\left(\sigma\frac{\partial D}{\partial x_1} + \frac{\partial \eta}{\partial x_1}\right)\psi_i\right]\right\} \tag{49}$$

$$q_2 = \mathrm{A_H}\frac{1}{h_2}\left\{\frac{\partial}{\partial x_2}(\psi_i D) - \frac{\partial}{\partial \sigma}\left[\left(\sigma\frac{\partial D}{\partial x_2} + \frac{\partial \eta}{\partial x_2}\right)\psi_i\right]\right\} \tag{50}$$

$$\begin{aligned} DF_q = &\frac{1}{h_1 h_2}\left\{\frac{\partial}{\partial x_1}(h_2 q_1) - h_2\frac{\partial}{\partial \sigma}\left[\left(\frac{\sigma}{D}\frac{\partial D}{\partial x_1} + \frac{1}{D}\frac{\partial \eta}{\partial x_1}\right)q_1\right]\right\} + \\ &\frac{\partial}{\partial x_2}\left\{(h_1 q_2) - h_1\frac{\partial}{\partial \sigma}\left[\left(\frac{\sigma}{D}\frac{\partial D}{\partial x_2} + \frac{1}{D}\frac{\partial \eta}{\partial x_2}\right)q_2\right]\right\} \end{aligned} \tag{51}$$

$$q_1 = \mathrm{A_H}\frac{1}{h_1}\left\{\frac{\partial}{\partial x_1}\left(q^2 D\right) - \frac{\partial}{\partial \sigma}\left[\left(\sigma\frac{\partial D}{\partial x_1} + \frac{\partial \eta}{\partial x_1}\right)q^2\right]\right\} \tag{52}$$

$$q_2 = \mathrm{A_H}\frac{1}{h_2}\left\{\frac{\partial}{\partial x_2}\left(q^2 D\right) - \frac{\partial}{\partial \sigma}\left[\left(\sigma\frac{\partial D}{\partial x_2} + \frac{\partial \eta}{\partial x_2}\right)q^2\right]\right\} \tag{53}$$

$$DF_l = \frac{1}{h_1 h_2}\left\{\frac{\partial}{\partial x_1}\left(h_2 q_1\right) - h_2\frac{\partial}{\partial \sigma}\left[\left(\frac{\sigma}{D}\frac{\partial D}{\partial x_1} + \frac{1}{D}\frac{\partial \eta}{\partial x_1}\right)q_1\right]\right\} + \frac{\partial}{\partial x_2}\left\{\left(h_1 q_2\right) - h_1\frac{\partial}{\partial \sigma}\left[\left(\frac{\sigma}{D}\frac{\partial D}{\partial x_2} + \frac{1}{D}\frac{\partial \eta}{\partial x_2}\right)q_2\right]\right\} \tag{54}$$

$$q_1 = \mathrm{A_H}\frac{1}{h_1}\left\{\frac{\partial}{\partial x_1}\left(q^2 lD\right) - \frac{\partial}{\partial \sigma}\left[\left(\sigma\frac{\partial D}{\partial x_1} + \frac{\partial \eta}{\partial x_1}\right)q^2 l\right]\right\} \tag{55}$$

$$q_2 = \mathrm{A_H}\frac{1}{h_2}\left\{\frac{\partial}{\partial x_2}\left(q^2 lD\right) - \frac{\partial}{\partial \sigma}\left[\left(\sigma\frac{\partial D}{\partial x_2} + \frac{\partial \eta}{\partial x_2}\right)q^2 l\right]\right\} \tag{56}$$

Boundary conditions

On the free surface and considering that the sigma coordinate model is selected: $z = \eta\left(x_1, x_2\right)$, the speed won the surface will be calculated as follows:

$$\mathrm{w} = \frac{\partial \eta}{\partial \mathrm{t}} + \mathrm{u}_1\frac{\partial \eta}{\partial x_1} + \mathrm{u}_2\frac{\partial \eta}{\partial x_2} \tag{57}$$

The momentum flux of the oil spill is shown with (57-58) equations:

$$\begin{aligned}\mathrm{K_M}\left(\frac{\partial u_1}{\partial z}, \frac{\partial u_2}{\partial z}\right) &= \frac{1}{\rho 0}\left(\tau_{01}, \tau_{02}\right)\\ \mathrm{K_M}\left(\frac{\partial \dot{\mathrm{E}}}{\partial z}, \frac{\partial S_i}{\partial z}\right) &= \frac{1}{\rho_0}\left(\overline{Q_H}, \overline{Q_{S_i}}\right)\end{aligned} \tag{58}$$

The $\mathrm{K_M}$ is the effect of wind stress on the sea surface and heat flux. The oil spill flux on the ocean's surface interacts with various energy forms. This includes the heat flux of long and short solar radiation waves that bounce off the sea surface, as well as the sea's latent and sensible heat flux exchanged with the atmosphere. This balance is achieved through: $\tau_{01}\tau_{02}\overline{Q_H}\overline{Q_{S_i}}\overline{Q_H}$

Where τ_{01} and τ_{02} are the effect of wind stress on the sea surface and $\overline{Q_H}$ is the heat flux and $\overline{Q_{S_i}}$ is the oil spill flux entering the sea surface. $\overline{Q_H}$, which is the heat flux, is obtained by a balance of different energies such as long and short waves of solar radiation and back radiation from the sea surface and the latent and sensible heat flux of the sea to the atmosphere, which is obtained as:

$$\overline{Q_H} = \overline{\beta}\left(1-\overline{\alpha}\right)S_W + L_W - \varepsilon\overline{\sigma}\mathrm{T}_S^4 - \mathrm{H}s - \mathrm{H}_L \tag{59}$$

In the relation above, S_W is the flux of short waves of solar radiation and L_W is the flux of long waves of solar radiation and $\overline{\alpha}$ is the flux of return radiation from the sea surface and ε is the diffusion coefficient and $\overline{\sigma}$ is Stefan Boltzmann's constant and T_S is the temperature of the sea surface and Hs is the sensible heat flux and H_L is the latent heat flux Are. And of course, $\overline{\beta}$ is the absorption coefficient of the sea surface. To calculate the oil spill flux, the relation is:

$$\overline{Q_S} = S_s\left(\dot{E} - \dot{P}\right) \tag{60}$$

Where $\dot{E}$ the intensity of evaporation and $\dot{P}$ is the intensity of precipitation on the sea surface and S_s is the area of the oil spill which known as:

$$(\Theta, S_i) = (T_S, S_S) \tag{61}$$

The following relation for time delay t_l

$$\frac{\partial}{\partial t}(\Theta, S_i) = -\frac{1}{t_l}[(\Theta - T_S), (S - S_S)] \tag{62}$$

Which will be a suitable estimate for simulating weather conditions on the sea surface. For the turbulent flow over the free surface of the sea, we assume that the sea waves do not create turbulence near the surface. Therefore, the following relation is:

$$q^2 = \mathrm{B}_1^{2/3}{u_{*0}}^2 \quad and \quad l = 0 \tag{63}$$

Where u_{*0} the friction is speed on the sea surface and is calculated from the following equation:

$$u_{*0} = \left[\frac{\tau_{01}^2 + \tau_{02}^2}{\rho_{01}^2}\right]^{\frac{1}{4}} \tag{64}$$

For the boundary conditions of the seabed and considering that the sigma coordinate model in the sea bed *Z*= -H is assuming that we do not have any mass flow into the sea, then the speed w will be calculated from the following equation:

$$\left(\frac{\partial\Theta}{\partial z}, \frac{\partial S_i}{\partial z}\right)_b = (0, 0_i) \tag{65}$$

$$\omega = -u_{1b}\frac{\partial \mathrm{H}}{\partial x_1} - u_{2b}\frac{\partial \mathrm{H}}{\partial x_2} \tag{66}$$

So momentum flux and buoyancy like heat flux and oil spill and turbulent flow are shown by the following relations:

$$\mathrm{K_M}\left(\frac{\partial u_1}{\partial z},\frac{\partial u_2}{\partial z}\right)=\frac{1}{\rho_0}\left(\tau_{b1},\tau_{b2}\right) \tag{67}$$

$$q^2=\mathrm{B}_1^{2/3}u_{*b}^2 \quad and \quad l=0 \tag{68}$$

$$u_{*b}=\left[\frac{\tau_{b1}^2+\tau_{b2}^2}{\rho_{01}^2}\right]^{\frac{1}{4}} \tag{69}$$

Certainly, the calculation of stress on the seabed is derived using a logarithmic formula based on the velocities u_1b and u_2b at the location z_b, as demonstrated below:

$$\left(\tau_{b1},\tau_{b2}\right)=\rho_0 C_D\left[u_{1b}^2+u_{2b}^2\right]^{1/2}\left(u_{1b},u_{2b}\right) \tag{70}$$

$$C_D=\left[\frac{1}{\kappa}\ln\left(\frac{\mathrm{H}+z_b}{z_0}\right)\right]^{-2} \tag{71}$$

Where C_D the drag coefficient and its values is are considered 0.0025, z_0 is the magnitude of roughnessOn the coast, it is presumed that there are factors like mass flow, momentum flux, and buoyancy, which include elements such as heat flux, oil spills, and turbulent flows. Conversely, when dealing with a river, the boundary conditions at the river mouth assume that the current flows perpendicular to the coastline, affecting both momentum and buoyancy flux.:

$$\frac{\partial}{\partial t}(\Theta,S_i)+u_n\frac{\partial}{\partial n}(\Theta,S_i)=0 \tag{72}$$

In this context, “n” denotes the line perpendicular to the coastline. Notably, we refrain from setting boundary conditions for turbulent flow to ensure precise calculations. Another point to consider is the state of the free boundary. For instance, if the examining a specific sea region, like the southern part of Makran’s coast, it has no define for certain conditions without information about the external boundary. This becomes even difficult when focusing on internal aspects, as highlighted by (LH Kantha et al.,1990).

$$\frac{\partial\phi}{\partial t}+c\frac{\partial\phi}{\partial\eta}=0 \tag{73}$$

that the parameter ϕ can be factors such as η, u_1, u_2, etc. and c is the phase speed inside the boundary.

GNOME model

The GNOME model uses the CATS (Current Analysis for Trajectory Simulations) hydrodynamic model by default. However, it is possible to use other hydrodynamic models such as the nowcast/forecast circulation model. The CATS model is a two-dimensional depth-averaged finite element circulation model. CATS generates static patterns that depend on GNOME and correlate it with a time series, such as tidal coefficients. These patterns are generated relatively quickly and are easily adjusted during the response. These patterns are in a triangular grid, which enables higher resolution and good matching near the coasts.

For example, tides are represented in most location files as $\vec{U}(x.y)\vec{T}(t)$. CATS uses a spatial pattern of $\vec{U}_{CATS}$ for the currents and then the NOAA tidal current time series for the nearest

tide station to adjust the currents back and forth. Therefore, for a station at the point $x_0.y_0$, the current at each point $\vec{U}(x.y)$ is obtained by the following relation (B. Zelenke et al.,2012):

$$\vec{U}(x.y) = \vec{T}(x_0.y_0.t) * \frac{\vec{U}_{CATS}(x.y)}{\vec{U}_{CATS}(x_0.y_0)} \quad (74)$$

Extraction of physical data of Makran region and oil spill spreading places

Flow data includes water flow data, etc., which depends on time. This information was obtained from NOAA's Real-Time Ocean Forecast System (RTOFS) and the information was extracted for a period of 90 days (2160 hours) from the starting date of January 1(December 22, 2022). The extracted area is shown in Figure 1. Also, four different places are considered for spreading the oil stain, whose coordinates and locations are shown in Figure 2 and Table 1. The type of oil is Medium Crude Oil and 1000 Liter is released in those places. The calculation time is per hour.

RESULTS AND DISCUSSION

Mesh creation and mesh independence calculations

In this research, the skewness value was used to evaluate the quality of the mesh. The meshing was done in such a way that the average skewness obtained was 0.7911, which is in the range of excellent meshing quality. The number of meshes was 386,962. Figures 3 and 4

Table 1. Coordinates of oil release points

The number of the place of release	GIS
P1	25.383166, 59.351833
P2	25.246833, 60.53233
P3	24.99233, 61.578
P4	25.012833, 62.315833

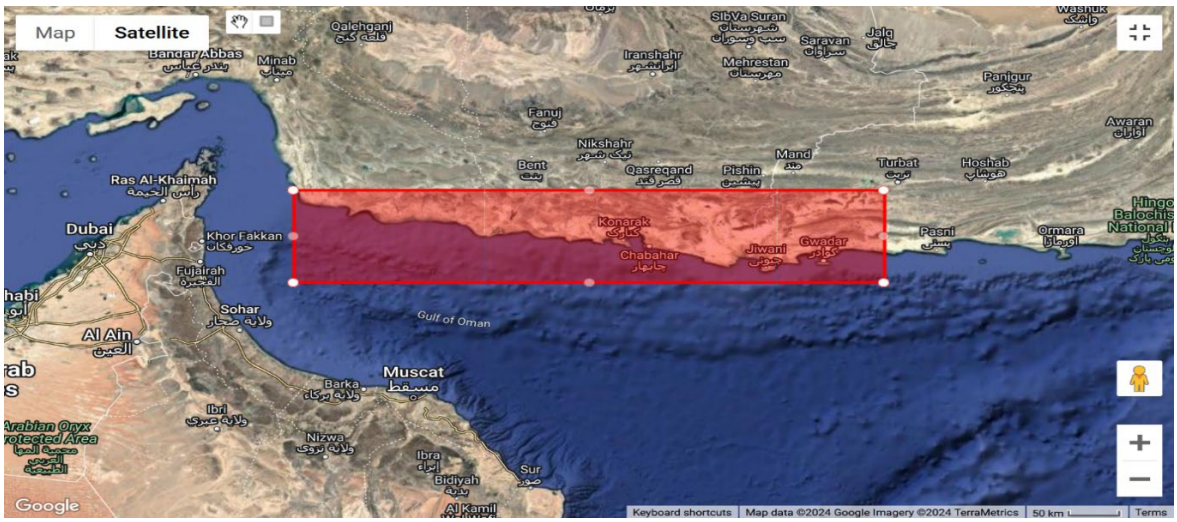

Fig. 1. Flow data extraction area for Makran area for a period of 90 days from January 1, 2022, left Top (25.922, 57.225) and right bottom (24.89, 62.912)

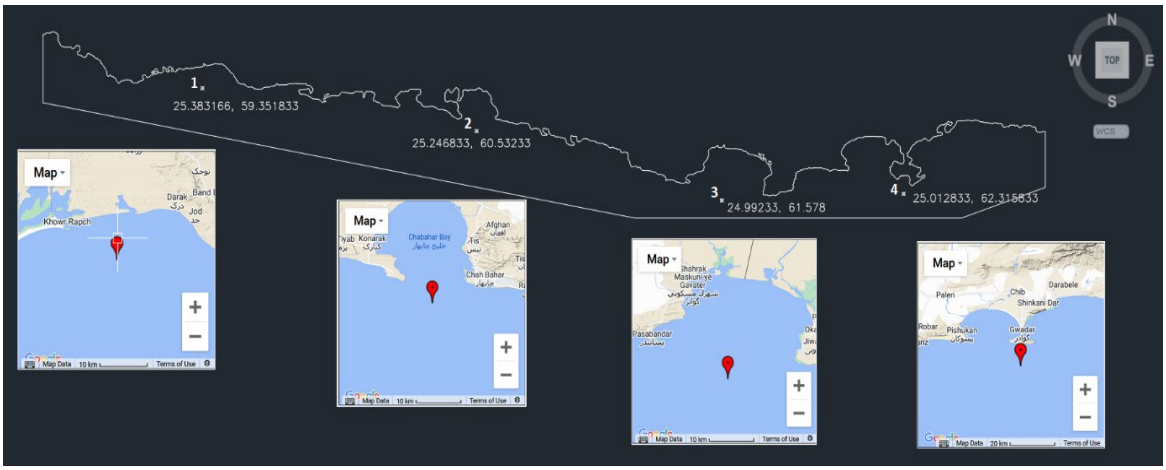

Fig. 2. Coordinates of crude oil release (points) locations (P1, P2, P3 and P4)

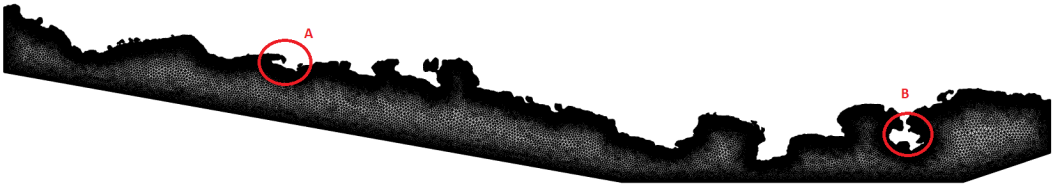

Fig. 3. Mesh of geometry for Makran area

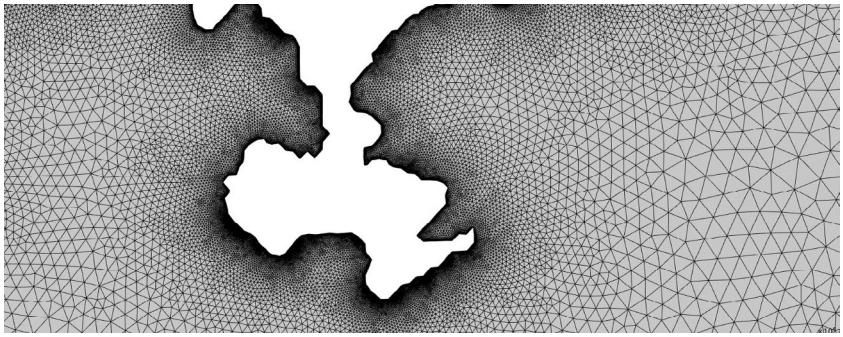

Fig. 4. Example of zone meshing, geographic coordinates of the center is 25.0785, 62.3271

show the selected area of Makran after applying the mesh.

To determine the height of each section of the mesh, the process begins by converting coordinates into data points. These points reflect the depth of the specific area being studied and are fed into a support vector machine (SVM) as a learning dataset. Following this, newly generated mesh points are inputted into the SVM system to compute the depth of each individual mesh point. And finally, the depth of each triangular column of the unstructured mesh will be the average depth of a triangle vertex.

The skewness value indicates that the mesh is suitable; however, the number of mesh elements can impact the precision of the results. To investigate this, the model is run over the first 24 hours to simulate the spreading of an oil spill, using different mesh counts. The calculations focus on the spill's area, measured in square kilometers. This work was done for all four points as shown in Figure 2, and the results are shown in Table 2. According to the results of this table, the number of meshes is 386,962.

Table 2. Numerical solution results to calculate the independence of the mesh in terms of the spread area of the oil spill with the number of different meshes

The number of meshes	Area of the oil stain at point 1	Area of the oil stain at point 2	Area of the oil stain at point 3	Area of the oil stain point 4
268632	2.8658	2.5623	2.6957	2.5684
312448	3.1325	2.8079	2.8035	2.6895
386962	**3.1335**	**2.8134**	**2.8089**	**2.6923**

Numerical solution results for crude oil release points

As mentioned in the previous section, flow data were extracted for numerical solutions over a period of 90 days (2160 hours) starting from January 1 to December 22, (2022). For the numerical solution of each hour out of the total 2160 hours, 360 repetitions were conducted across all meshes, resulting in 776,600 loops for each cell of the 386,962 meshes at each of the four oil release points. In total, 300,901,651,200 loops were executed, with momentum equations solved in each iteration. Each layer also included an inner ring within the sigma layer. The numerical calculations for each release point required approximately 23 days of processing time (92 days total) on a computer with an Intel(R) Core(TM) i7-7500U CPU @ 2.70GHz.

Figure 2 is illustrated the four selected release points: Point 1 was positioned along a relatively flat coastline; Points 2 and 3 were near the entrance of the bay; and Point 4 lay between two bays. Figure 5 represents release point 1, Figure 6 shows point 2, Figure 7 depicts point 3, and Figure 8 illustrates point 4. Due to the extensive coastal border, currents from the Strait of Hormuz had a more pronounced effect on release point 1 than on the distant points. As shown in Figure 5, a hypothetical oil spill at point 1 would, over three months, affect a significant portion of Makran's coastal area (around two-thirds), ultimately reaching the coastline. Figures 6, 7, and 8 show that the oil spread at points 2, 3, and 4 predominantly impacted the inner coastlines of the Gulf, with a limited effect on other parts of the Makran coast. The spread at point 4, being closer to the ocean,

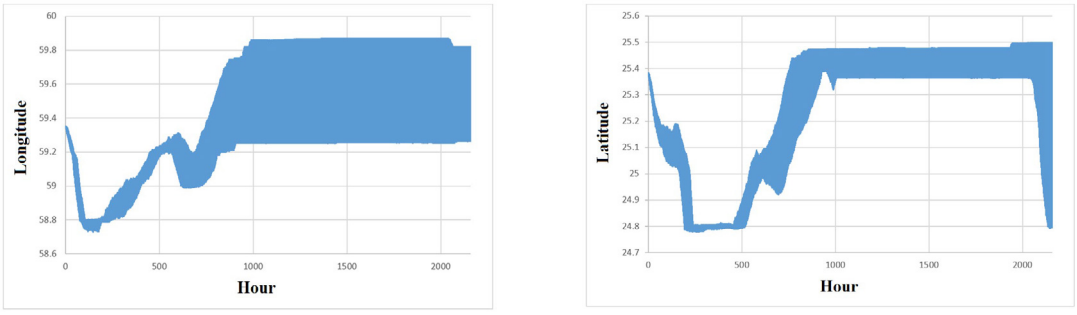

(b) (a)

Fig. 5. Variations of geographical latitude (a) and longitude (b) of the oil spill with respect to the hour for point 1

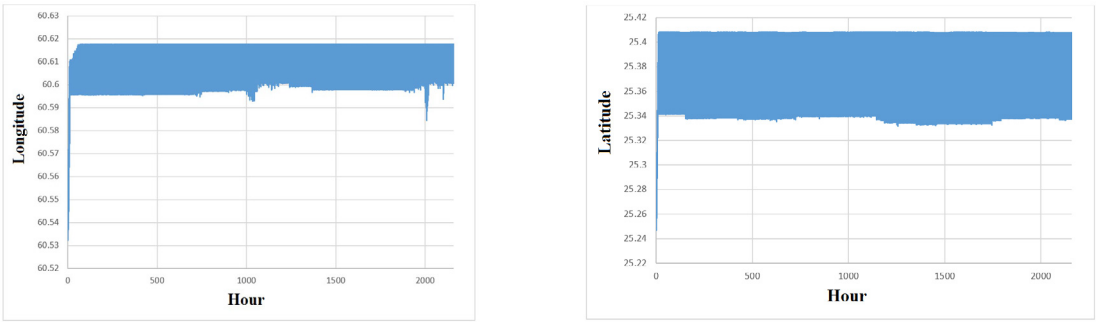

(b) (a)

Fig. 6. Variations of geographical latitude (a) and longitude (b) of the oil spill with respect to the hour for point 2

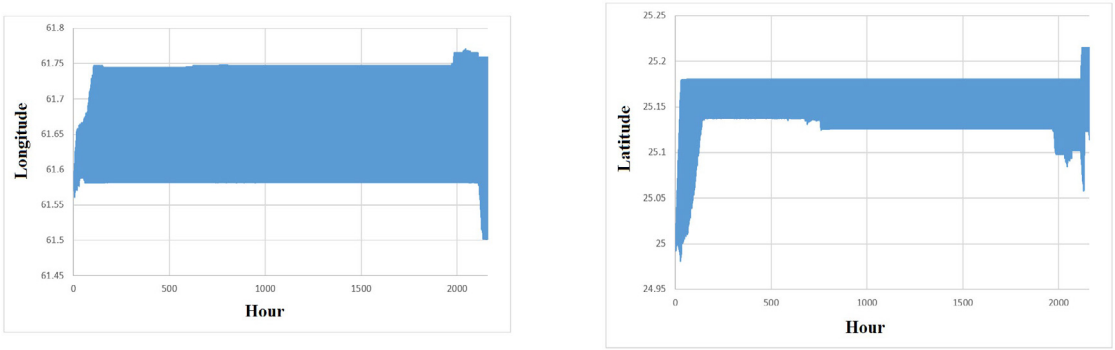

(b) (a)

Fig. 7. Variations of geographical latitude (a) and longitude (b) of the oil patch with respect to the hour for point 3

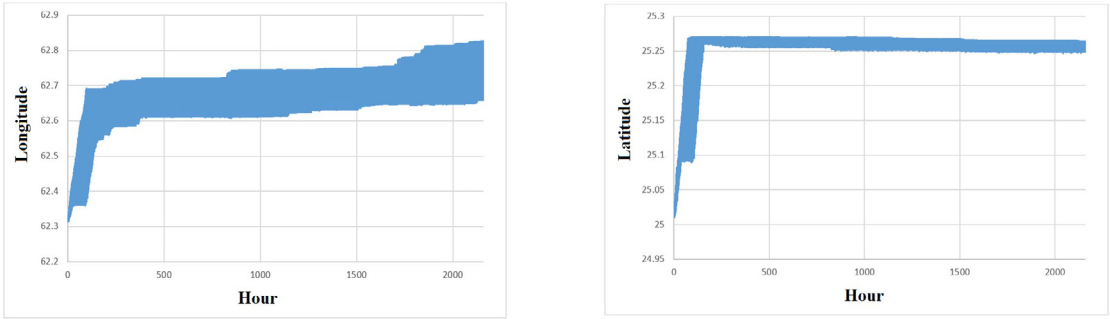

(b) (a)

Fig. 8. Variations of geographical latitude (a) and longitude (b) of the oil spill with respect to the hour for point 4

extended rightward, impacting the coast of Pakistan rather than the Gulf's left side.

This study determined the fate of the oil spill using the finite volume method for 90 days (2160 hours) starting from January 1to December 22, 2022 across four release locations as shown in Figure 2, with coordinates listed in Table 1. The released oil was 1000 liters of Medium Crude Oil. Initial conditions, including flow data from NOAA, were utilized in this three-month simulation period. Based on these initial conditions and coordinates, GNOME software was used to calculate the oil spill distribution. Figures 9 to 12 illustrated the results for each release site, showing the oil spill's progression after three months. In these figures, the release location is marked by a (+), red dots represent oil with low concentration, and black dots signify undissolved crude oil at its initial concentration.

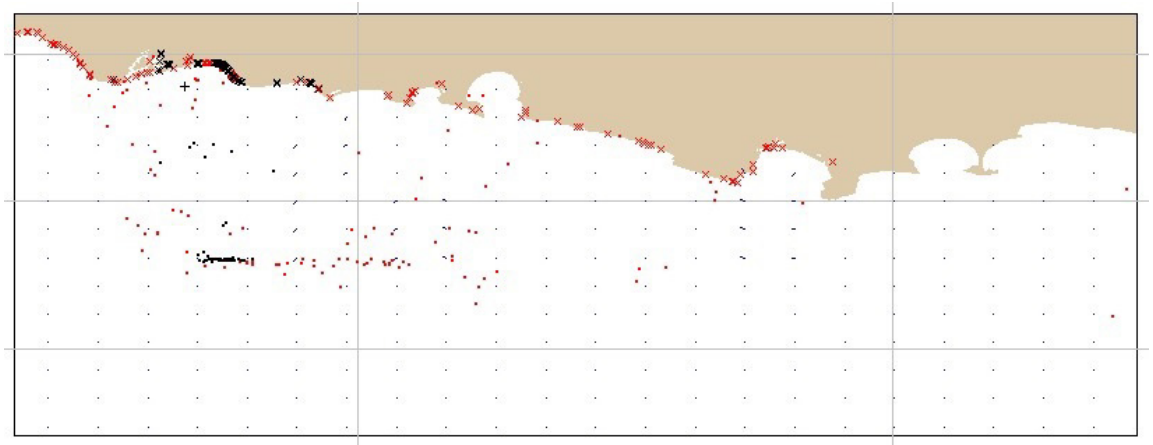

Fig. 9. The fate of the oil spill three months after release for point 1

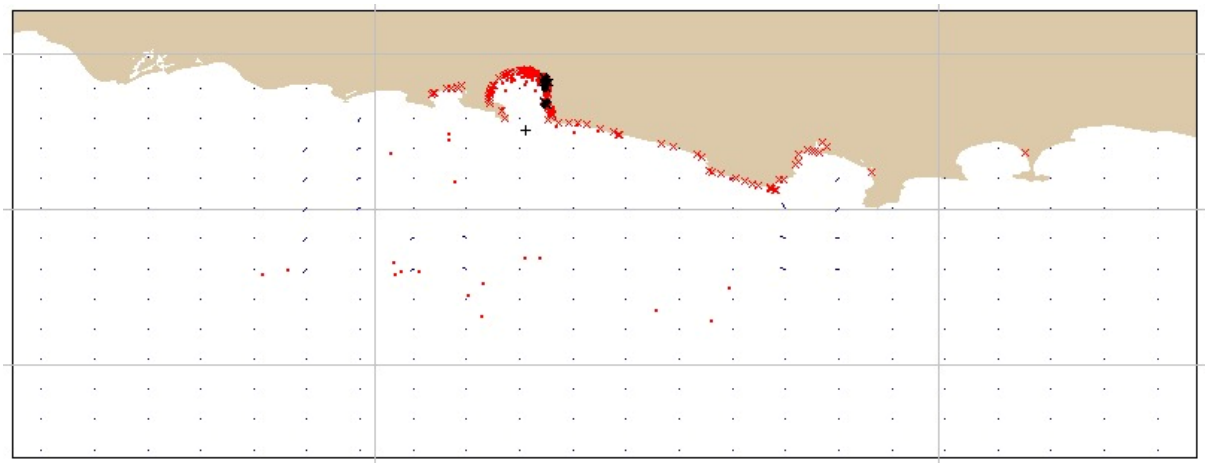

Fig. 10. The fate of the oil spill three months after release for point 2

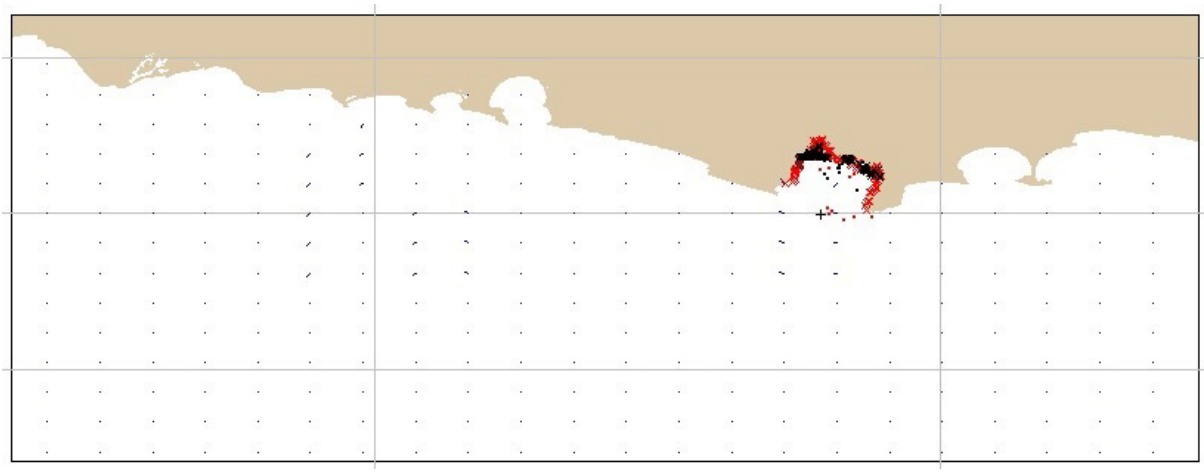

Fig. 11. The fate of the oil spill three months after release for point 3

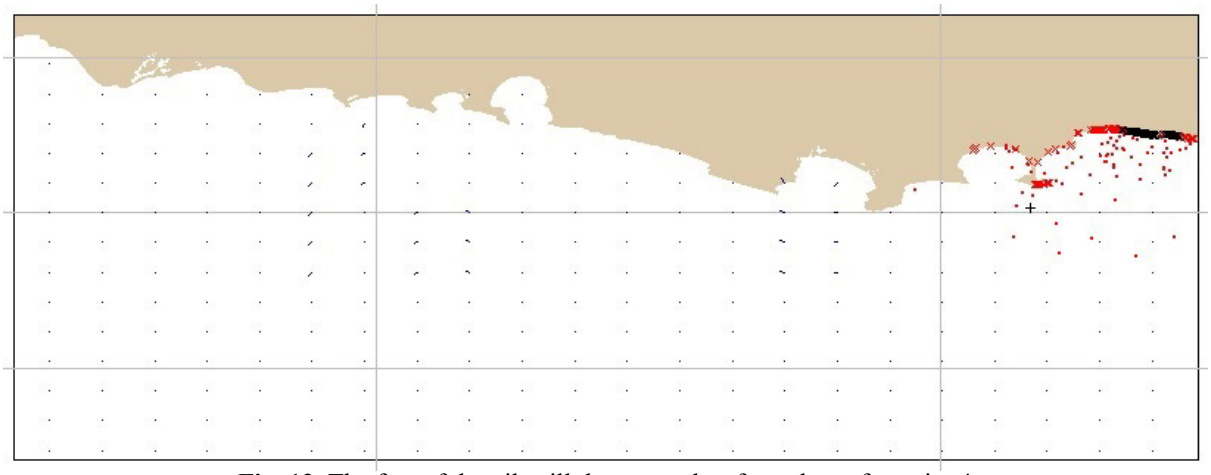

Fig. 12. The fate of the oil spill three months after release for point 4

CONCLUSION

The finite volume model showed that currents from the Strait of Hormuz had a stronger impact on the spread from point 1 compared to other locations that are further away. If there were an oil spill at point 1, it would mostly affect the Makran coastal region, covering about two-thirds of it within three months, eventually reaching the shoreline. For points 2 and 3, the spread reached inner coastlines within the bay, with only a limited impact on other areas of the Makran coast. At point 4, since it's close to the ocean, the spread moved toward the coast of Pakistan instead of going to the left side of the Gulf, as shown in Figures 9 to 12 using GNOME.

Figure 13 showed the results for 7-day intervals, and the table 3 is clarified the three-months average percentage differences. The oil is dispersed within coastline in point 1 hence in point 3 the contamination is accumulated around the bay and the dispersion is the less compare to the point 1,2, 4. A direct numerical comparison between two methods Finite volume modeling and GNOME was challenging, as GNOME software models the initial oil spill as a defined set of points that move along the water surface during the simulation, rather than using a mesh-based approach. However, both methods adopted similar principles to the Sigma approach used in this research. For comparison, a scoring method was applied: coordinates of distributed points were obtained from GNOME at set intervals and matched against the mesh results from the finite volume model. If oil was detected within the corresponding mesh, a point was added to the total, yielding a percentage of matched points. The second and third points affected the inside the bay coast, while the fourth point showed pollution spreading toward out the bay toward the Pakistan's coast. The coastline around the bay is clarified by the model result and the calculation as the highest risk areas according to the bay curve morphology coast, currents, wind and other atmospheric parameters which impacted the spill motion.

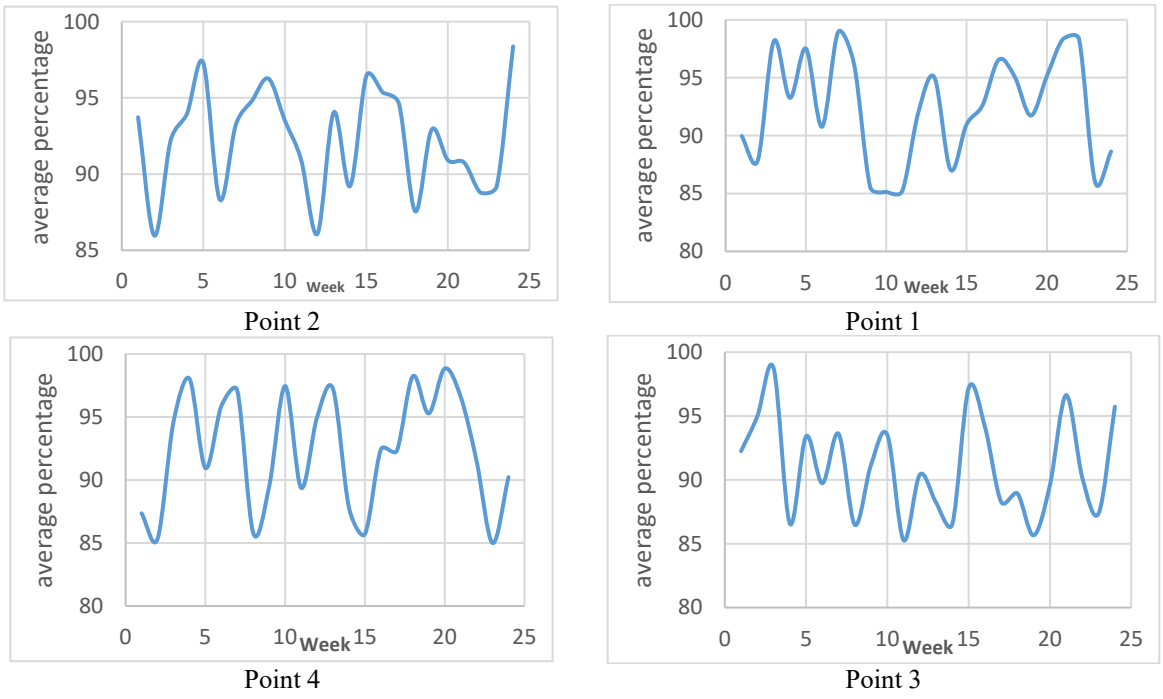

Fig. 13. The percentage difference between the results of finite volume method and GNOME

Table 3. The average percentage of the difference between the results of finite volume method and GNOME in the period of three months for released points (P1, P2, P3 and P4)

The number of the place of release	Average percentage difference
P1	92.33
P2	92.28
P3	91.03
P4	92.40

GRANT SUPPORT DETAILS

The present research did not receive any financial support.

CONFLICT OF INTEREST

The authors declare that there is not any conflict of interests regarding the publication of this manuscript. In addition, the ethical issues, including plagiarism, informed consent, misconduct, data fabrication and/ or falsification, double publication and/or submission, and redundancy has been completely observed by the authors.

LIFE SCIENCE REPORTING

No life science threat was practiced in this research.

REFERENCES

Abascal, AJ., Castanedo, S., Medina, R., & Liste, M. (2010). Analysis of the reliability of a statistical oil spill response model. Marine Pollution Bulletin, 60(11), 2099 -2110.

Abbasi, H., & Lubbad, R. (2021). A numerical model for the simulation of oil–ice interaction.Physics of Fluids, 33(10), 102-117.

Afenyo, M., Veitch, B., & Khan, F. (2016). A state-of-the-art review of fate and transport of oil spills in open and ice-covered water. Ocean Engineering, 119, 233-248.

Agrawal, M., & Dakshinamoorthy, D. (2011). Computational analysis of oil spill in shallow water due to wave and tidal motion. inOffshore Technology Conference, Houston, TX, 2-5.

Ahrari Roudi, M.A. (2021). Overview of pollutants in the Oman Sea and its effects on the marine ecosystem. Shipping and Marine Technology, 5(4), 21-30.

Basar,E., Kose,E., & Guneroglu,A.(2006). Finding risky areas for oil spillage after tanker accidents at Istanbul strait. International journal of environment and pollution, 27(4), 388- 400.

Camp,JS., LeBoeuf,EJ., & Abkowitz,MD. (2010). Application of an enhanced spill management information system to inland waterways. Journal of Hazardous Materials 175(1-3), 583-592.

Chao, X., NJ Shankar., & HF Cheong. (2001). Two-and three-dimensional oil spill model for coastal waters. ocean engineering 28(12),1557-1573.

Drozdowski,A., Nudds,S., Hannah,G.G., Niu,H., Peterson,I.K., & Perrie,W.A.(2011).

Review of oil spill trajectory modeling in the presence of ice. DFO, Dartmouth, NS(Canada), 0711-6764.

Elliott,AJ.(1986). Shear diffusion and the spread of oil in the surface layers of the North Sea. Deutsche Hydrografische Zeitschrift, 39(3), 113-137.

Farzingohar, M., Bagheri, M., Golami, I., & Zaiton, Z.(2024). Mapping pollution dynamics: utilizing

GNOME to model oil spill trajectories in tanker terminals. Environmental Science and Pollution Research, 31, 37404-37427.

Fay, JA.(1969). The spread of oil spills on a calm sea. in Oil on the Sea: Springer, 53-63.

Fingas, M.(2002).The basics of oil spill cleanup. CRC press.

Fraga Filho., CAD.(2021). A Lagrangian analysis of the gravity-inertial oil spreading on the calm sea using the reflective oil-water interface treatment. Environmental Science and Pollution Research, 28(14), 17170-17180.

French-McCay, DP., Tajalli-Bakhsh., T, Jayko., K, ML Spaulding., & Li,Z.(2017). Validation of oil spill transport and fate modeling in Arctic ice. Arctic Science, 4(1), 71-97.

Galperin,B., Kantha,L., Hassid,S., & Rosati,A.(1988). A quasi-equilibrium turbulent energy model for geophysical flows. Journal of the atmospheric sciences, 45(1).

Ha,C-T & Lee, JH.(2020). A modified monotonicity-preserving high-order scheme with application to computation of multi-phase flows. Computers & Fluids, 197, 104345.

Hoang, AT., Pham, VV., & Nguyen DN.(2018). A report of oil spill recovery technologies. Int. J. Appl. Eng. Res, 13(7), 4915-4928.

JM, Sayol., Orfila, A., Simarro, G., Conti, D., Renault, L., & Molcard, A.(2014). A Lagrangian model for tracking surface spills and SaR operations in the ocean. Environmental modeling & software,52, 74-82.

Kantha, LH., Blumberg,AF., & Mellor,GL.(1990). Computing phase speeds at open boundary. Journal of Hydraulic Engineering, 116(4), 592-597.

Lehr,W., Jones, R., Evans, M., Simecek-Beatty, D., & Overstreet, R.(2002). Revisions of the ADIOS oil spill model. Environmental Modeling and Software, 17(2), 189-197.

Mackay, D., Shiu, WY., Hossain,K., Stiver,W., & McCurdy,D.(1982). Development and Calibration of an Oil Spill Behavior Model.Toronto Univ (ONTARIO) Dept of Chemical Engineering and Applied Chemistry.

Mellor, GL & Yamada, T.(1982). Development of a turbulence closure model for geophysical fluid problems. Reviews of Geophysics, 20(4), 851-875.

Mellor, GL., SM, Häkkinen., Ezer, T., & RC Patchen.(2002). A generalization of a sigma coordinate ocean model and an intercomparison of model vertical grids. in Ocean forecasting: Springer, 55-72.

Qiao., F et al.(2019). Modeling oil trajectories and potentially contaminated areas from the Sanchi oil spill. Science of the Total Environment, 685, 856-866.

Raznahan, M., An, C., SS, Li., Geng, X., & Boufadel, M.(2021). Multiphase CFD simulation of the nearshore spilled oil behaviors. environmental pollution, 288, 117730.

Silva, NR., & Manssour, IH.(2007). A curvilinear cutting tool for the analysis of oceanography data.

Simecek, D-Beatty., & Lehr,WJ.(2007). Trajectory modeling of marine oil spills. Oil spill environmental forensics, 405-418.

Smith, R et al.(2014). Oceanographic conditions in the Gulf of Mexico in July 2010, during the Deepwater Horizon oil spill. Continental Shelf Research, 77, 118-131.

Sugioka, S.i., Kojima, T., Nakata, K., & Horiguchi, F.(1999). A numerical simulation of an oil spill in Tokyo Bay. Spill Science & Technology Bulletin, 5(1), 51-61.

Tkalich, P.(2006). A CFD solution of oil spill problems. Environmental Modeling & Software, 21(2), 271-282.

Venkatesh, S., El-Tahan, H., Comfort, G., & Abdelnour, R.(1990). Modelling the behavior of oil spills in ice-infested waters. Atmosphere-Ocean, 28(3), 303-329.

Wang, S., Shen, Y., & Zheng,Y.(2005). Two-dimensional numerical simulation for transport and fate of oil spills in seas. Ocean Engineering, 32(13), 1556-1571.

Yang, M., Khan, F., Garaniya, V., & Chai, S.(2015). Multimedia fate modeling of oil spills in ice-infested waters: An exploration of the feasibility of fugacity-based approach. Process Safety and Environmental Protection. 93, 206-217.

Yousefi Kobriya, D., Abbaskhanian, G., & Ghanbari Parmehar, A.(2020). Identification of oil pollution spots in the Caspian Sea using remote sensing (case study: Baku oil extraction facilities). Environmental Sciences Quarterly. 18(3), 152-166.

Zahed, M.AM., Rouhani, F., Mohajeri, S., Bateni, F., & Mohajeri, L.(2010). An overview of Iranian mangrove ecosystems, northern part of the Persian Gulf and Oman Sea. Acta Ecologica Sinica, 30(4), 240-244.

Zelenke, B., O'Connor, C., Barker, C.H., Beegle-Krause, C., & Eclipse, L.(2012). General NOAA operational modeling environment (GNOME) technical documentation.

Zhang, Z., Kress, ME., & Schäfer, T.(2020). A lattice boltzmann advection diffusion model for ocean oil spill surface transport prediction. in2020 Winter Simulation Conference (WSC), IEEE, 680-691.